ELSEVIER

Vanadium and molybdenum disorder in $M_{2.5}VMoO_8$ (M = Mg, Mn, and Zn) determined with neutron powder diffraction and phase formation studies of $Mg_{2.5+x}V_{1+2x}Mo_{1-2x}O_8$

Xiandong Wang [a], Jason D. Pless [a], Douglas A. Vander Griend [a], Peter C. Stair [a],
Kenneth R. Poeppelmeier [a,*], Zhongbo Hu [b], James D. Jorgensen [b]

[a] *Department of Chemistry, Northwestern University, Evanston, IL 60208-3113, USA*
[b] *Argonne National Laboratory, Building 223, Argonne, IL 60439-4814, USA*

Abstract

Disorder between the vanadium and molybdenum sites was investigated using neutron diffraction on polycrystalline samples of $M_{2.5}VMoO_8$ (M = Mg^{2+}, Mn^{2+}, Zn^{2+}) and the distribution of V^{5+} and Mo^{6+} among the tetrahedral sites was determined to be nearly statistical. The refined structures for all three polycrystalline samples corroborate those of corresponding single crystals determined previously with X-ray single crystal diffraction. Studies directed at the formation of $Mg_{2.5+x}V_{1+2x}Mo_{1-2x}O_8$ ($x = 0$, ± 0.02 and ± 0.04) demonstrate that the phase begins to form at an appreciable rate at 1173 K, which is approximately 250 K below its melting point.
© 2004 Elsevier B.V. All rights reserved.

Keywords: Vanadate; Molybdate; Neutron diffraction; Cation vacancies

1. Introduction

The selective oxidative dehydrogenation (ODH) of light hydrocarbons has become an important area of research for the petrochemical and energy industries. Owing to yields that are at best marginal, selective oxidation of alkanes is among the most challenging of catalytic problems. Mixed metal oxides with vanadium and molybdenum in isolated MO_4 tetrahedra, such as $Mg_3(VO_4)_2$ and $MgMoO_4$, are active in the selective ODH of low molecular weight alkanes [1–6]. $Mg_{2.5}VMoO_8$, a mixed Mg–V–Mo metal oxide, has been shown to have selectivities and activities for the ODH of propane and butane that are similar to those of $Mg_3(VO_4)_2$ [7,8].

The structures of a variety of analogous solid solution compounds $M_{2.5+x}V_{1+2x}Mo_{1-2x}O_8$ (M = Mg^{2+}, Mn^{2+}, Zn^{2+}; $-0.15 < x < 0.15$) have been determined previously by single crystal X-ray diffraction (XRD) at 153 K [9–12]. The oxidation states of vanadium and molybde-

num remain unchanged in these remarkable structures [7]. Electrical neutrality is maintained by the partial and variable occupancy of the divalent cations. In all cases, X-ray diffraction (XRD) indicated that the V^{5+} and Mo^{6+} cations were completely disordered among all the tetrahedral sites, however, the occupancies were not obtained directly from least squares refinements. The V/Mo cations in such vanadium–molybdenum-oxides as $K_{0.13}V_{0.13}Mo_{0.87}O_3$ [13], $NaVMoO_6$ [14], $Mn_{0.47}V_{0.94}Mo_{1.06}O_6$ [15] and $V_{1.44}Mo_{0.56}O_5$ [16] are also assumed to be statistically disordered based on X-ray diffraction experiments.

Precisely characterizing the disorder of the vanadium and molybdenum in such compounds is important because their distribution among the tetrahedral sites affects both the particular M^{2+} cation-sites where vacancies occur and the discrete tetrahedra themselves. These individual tetrahedra, which comprise the bulk structure, are believed to be an essential component in the stabilization of the surface(s) important in heterogeneous catalysis. Neutron diffraction can be used to ascertain definitively the cation distribution in crystalline solids. It is particularly useful for V/Mo disorder problems because vanadium is effectively invisible to the neutron beam. The coherent scattering length, b, of

* Corresponding author. Tel.: +1-847-491-3505;
fax: +1-847-491-7713.
E-mail address: krp@northwestern.edu (K.R. Poeppelmeier).

vanadium is negative ($b(V) = -0.3824(12)$ fm), while that for molybdenum is sizably positive ($b(Mo) = 6.715(20)$ fm) [17]. The investigation of the disorder of V^{5+} and Mo^{6+} in the title oxides with neutron diffraction is reported here for the first time.

In addition, uncertainty remains in the literature regarding the formation of $Mg_{2.5}VMoO_8$ and the temperature at which it forms, although its structure and catalytic properties have been reported [7,9,18]. López Nieto and co-workers reported that they were unable to detect the formation of $Mg_{2.5}VMoO_8$ in compositions of (mole percentage); 81.7, 4.7 and 13.6% and 87.8, 5.6 and 6.6% of MgO, V_2O_5 and MoO_3, respectively (where all of the MgO was the support phase) [19]. They detected three-phase mixtures of predominately MgO, and lesser amounts of $Mg_3(VO_4)_2$ and $MgMoO_4$ after the samples were calcined at 1173 K. As a result of the apparent discrepancy reported [19] for the preparation of $Mg_{2.5}VMoO_8$, a reinvestigation of the formation of this compound was undertaken.

2. Experimental

Polycrystalline $M_{2.5}VMoO_8$ (M = Mg, Mn, Zn) samples for neutron diffraction studies were prepared by solid state reaction of MgO (98%, Aldrich), Mn_2O_3 (99.9%, Aldrich), or ZnO (99.99%, Aldrich), with V_2O_5 (99.6%, Aldrich) and MoO_3 (>99.5%, Aldrich). Stoichiometric amounts of the appropriate oxides were ground in an agate mortar and ball-milled in an agate cylinder for approximately 30 min. $Mg_{2.5}VMoO_8$ was prepared by calcination at 903 K for 14 h in air in an Al_2O_3 crucible. The sample was then pressed into pellets and heated at 1173 K for 172 h and 1353–1373 K for 40 h in air on platinum foil. $Mn_{2.5}VMoO_8$ was prepared by calcination at 923 K for 12 h and then 953 K for 24 h. The sample was then ground, ball-milled and pressed into pellets before heating at 1023 K for 18 h and finally at 1173 K for 46 h in flowing argon. One intermittent grinding, ball-milling and pelletizing procedure was conducted during the last heat treatment. The inert atmosphere is necessary to control the oxidation state of manganese. $Zn_{2.5}VMoO_8$ was prepared by calcination at 923 K for 24 h in air in an Al_2O_3 boat. The sample was then pressed into a pellet and heated at 1073–1083 K for 90 h in air with one intermittent grinding, ball-milling and pelletizing procedure. The temperatures for the different heat treatments of the three samples were chosen to be approximately 35–110 K below their melting points [9–11]. Powder X-ray diffraction confirmed that all three samples were single phase.

Powder X-ray diffraction patterns were recorded at room temperature on a Rigaku diffractometer (Cu Kα radiation, Ni filter, 40 kV, 20 mA; $2\theta = 10–70°$, $0.05°$ step size and 1 s count time) and used for crystalline phase identification. The phases were identified by comparison with the data reported in the Joint Committee of Powder Diffraction Standards (JCPDS) database.

Table 1
Crystallographic data for $M_{2.5}VMoO_8$

Formula	$Mg_{2.5}VMoO_8$	$Mn_{2.5}VMoO_8$	$Zn_{2.5}VmoO_8$
Formula weight	335.64	412.23	438.36
Crystal system	Orthorhombic	Orthorhombic	Orthorhombic
Space group	$Pnma$	$Pnma$	$P2_12_12_1$
a (Å)	5.05355(5)	5.16413(5)	5.04316(6)
b (Å)	10.34326(9)	10.58043(9)	10.4054(1)
c (Å)	17.4613(2)	17.8711(2)	17.5657(2)
Z	6	6	6
d_{calc} (g/cm^3)	3.66	4.21	4.74
Variables	55	65	96
R_p	0.0363	0.0308	0.0311
R_{wp}	0.0509	0.0415	0.0440
χ^2	5.176	3.031	3.645

Powder neutron diffraction experiments were performed at the intense pulsed neutron source (IPNS) [20] at Argonne National Laboratory. Room temperature data (293 K) for all three compounds were recorded on the general purpose powder diffractometer. Low temperature (250, 150, 50 K) data for $Zn_{2.5}VMoO_8$ were recorded on the special environment powder diffractometer. Approximately 1 g of sample were loaded into cylindrical vanadium cans with sealed ends. Three pairs of detector banks with a total of 144 detectors, located at 150, 90 and 60° relative to the incident neutron beam, were used for data collection. The data collection for each sample required 12 h.

The data were analyzed using General Structure Analysis Software (GSAS) [21]. The unit cell parameters and atomic positions obtained from single crystal X-ray studies [9–11] were used as initial values for the refinements. In the final cycles of refinement, the unit cell parameters, atomic coordinates, an isotropic temperature factor for each atom as well as two terms of the Von Dreele–Jorgensen–Windor convolution peak shape function [22] were refined simultaneously against the intensities of 4196 observations. Only data from the high resolution back-scattering detector banks at 150° were used in the refinements. The crystallographic data and refined parameters are given in Table 1. The atomic positions and temperature factors for $Mg_{2.5}VMoO_8$, $Mn_{2.5}VMoO_8$ and $Zn_{2.5}VMoO_8$ are listed in Tables 2–4, respectively.

Samples of $Mg_{2.5+x}V_{1+2x}Mo_{1-2x}O_8$ ($x = 0$, ±0.02 and ±0.04) for thermal studies were prepared by a sol–gel method. The sol–gel method ensures a homogeneous mixture of the precursors, thereby lowering the calcination temperature generally required to overcome the kinetic limitations of solid-state diffusion. Stoichiometric amounts of magnesium ethoxide (Mg 21–22%, Alfa Aesar), vanadium triisopropoxide oxide (95–99%, Alfa Aesar) and bis(acetylacetonato)dioxomolybdenum(VI) (99%, Aldrich) were dissolved and refluxed in 2-methoxy ethanol (99%, Aldrich). The alkoxides were hydrolyzed with a 5% by volume NH_4OH aqueous solution. Upon hydrolysis, the samples precipitated from solution. After evaporation of the solvent, the precursors were dried at 383 K for 12 h. In one study, each of the five dried samples was calcined for 12 h

Table 2
Atomic parameters for $Mg_{2.5}VMoO_8$

Atom	Wyckoff	x	y	z	$100 \times U_{iso}$	Occupancy
V(1)	4c	0.215(1)	0.75	0.4428(2)	0.047(0.21)	0.516(9)
Mo(1)	4c	0.215(1)	0.75	0.4428(2)	0.047(0.21)	0.484(9)
V(2)	8d	0.7229(8)	0.4734(3)	0.3434(2)	1.2(2)	0.492(4)
Mo(2)	8d	0.7229(8)	0.4734(3)	0.3434(2)	1.2(2)	0.508(4)
Mg(1)	8d	0.7531(5)	0.5754(2)	0.5278(1)	1.13(7)	1
Mg(2)	4c	0.906(1)	0.75	0.2499(3)	3.6(1)	0.75
Mg(3)	4c	0.2555(7)	0.25	0.3025(2)	2.0(1)	1
O(1)	8d	0.9229(4)	0.3702(2)	0.2861(1)	1.68(8)	1
O(2)	8d	0.6534(4)	0.6134(2)	0.2960(1)	1.64(8)	1
O(3)	8d	0.9141(4)	0.5057(2)	0.4251(1)	1.41(7)	1
O(4)	8d	0.4344(4)	0.3856(2)	0.3721(1)	1.23(7)	1
O(5)	4c	0.9368(6)	0.75	0.5069(2)	0.91(9)	1
O(6)	8d	0.4137(5)	0.8853(2)	0.4649(1)	0.94(8)	1
O(7)	4c	0.1453(7)	0.75	0.3477(2)	1.2(1)	1

in air starting at 1148 K and the temperature was increased by 25 K every 12 h until the desired phase began to form. In a second study, the five dried precursors were calcined at 1173 K for varying time until the products were initially detected in the powder diffraction patterns.

Differential thermal analysis (DTA) measurements of the precursors, which had been dried at 383 K for 12 h, were made on a TA Instruments DSC 2910 Differential Scanning Calorimeter with platinum crucibles and alumina powder reference. The heating profiles consisted of linear ramps of 1, 2, 5 and 10 K min^{-1} from ambient temperature to 1373 K in a static air atmosphere. Before the measurements were made, the instrument was calibrated in the range of 430–1337 K to ensure accuracy.

3. Results and discussion

The final observed, calculated and difference profiles for $Mg_{2.5}VMoO_8$, $Mn_{2.5}VMoO_8$ and $Zn_{2.5}VMoO_8$ are shown in Figs. 1–3, respectively. The results confirm that all three polycrystalline $M_{2.5}VMoO_8$ (M = Mg^{2+}, Zn^{2+}, Mn^{2+})

samples at 293 K have the same structures as the corresponding single crystals at 153 K [9–11]. The Mg^{2+} and Mn^{2+} compounds are isostructural (*Pnma*). The bond connectivity in the Zn^{2+} analogue is identical, but distortions in the trigonal prismatic cation sites lead to a different space group ($P2_12_12_1$). The connectivity common to all three is illustrated in Fig. 4. All tetrahedral sites are occupied exclusively by either V^{5+} or Mo^{6+}. The V/MoO_4 tetrahedra link the trigonal prismatic $M^{2+}O_6$ and octahedral $M^{2+}O_6$ sites. The relatively large thermal displacement factors for Mg(2) (Table 2), Mn(2) (Table 3) and Zn(1) (Table 4) are a result of coulombic repulsions between adjacent divalent cations in the partially occupied (for $x = 0$ this site is occupied 75%) linear chains of face-shared octahedra. Many details of the structures have been described previously [9–11]. Selected bond distances and angles from the refinement of the neutron data for all three samples are given in Table 5. These results agree closely with those of the single crystal X-ray refinements [9–11].

To determine the disorder between vanadium and molybdenum, the relative site occupancies were refined under the following conditions: (i) the face-shared octahedral sites

Table 3
Atomic parameters for $Mn_{2.5}VMoO_8$

| Atom	Wyckoff	x	y	z	$100 \times U_{iso}$	Occupancy
V(1)	4c	0.222(1)	0.75	0.4415(3)	2.0(2)	0.47(1)
Mo(1)	4c	0.222(1)	0.75	0.4415(3)	2.0(2)	0.53(1)
V(2)	8d	0.7195(7)	0.4735(3)	0.3423(2)	1.2(1)	0.514(5)
Mo(2)	8d	0.7195(7)	0.4735(3)	0.3423(2)	1.2(1)	0.486(5)
Mn(1)	8d	0.7508(8)	0.5782(3)	0.5278(2)	2.02(8)	1
Mn(2)	4c	0.909(2)	0.75	0.2503(5)	4.6(2)	0.75
Mn(3)	4c	0.2565(9)	0.25	0.3023(3)	1.8(1)	1
O(1)	8d	0.9188(5)	0.3748(2)	0.2873(1)	2.36(6)	1
O(2)	8d	0.6550(4)	0.6093(2)	0.2975(1)	2.57(7)	1
O(3)	8d	0.9098(4)	0.5037(2)	0.4236(1)	2.06(6)	1
O(4)	8d	0.4447(4)	0.3861(2)	0.3706(1)	2.29(7)	1
O(5)	4c	0.9446(7)	0.75	0.5049(2)	2.14(8)	1
O(6)	8d	0.4112(5)	0.8815(2)	0.4632(1)	1.70(7)	1
O(7)	4c	0.1473(7)	0.75	0.3509(2)	2.7(1)	1
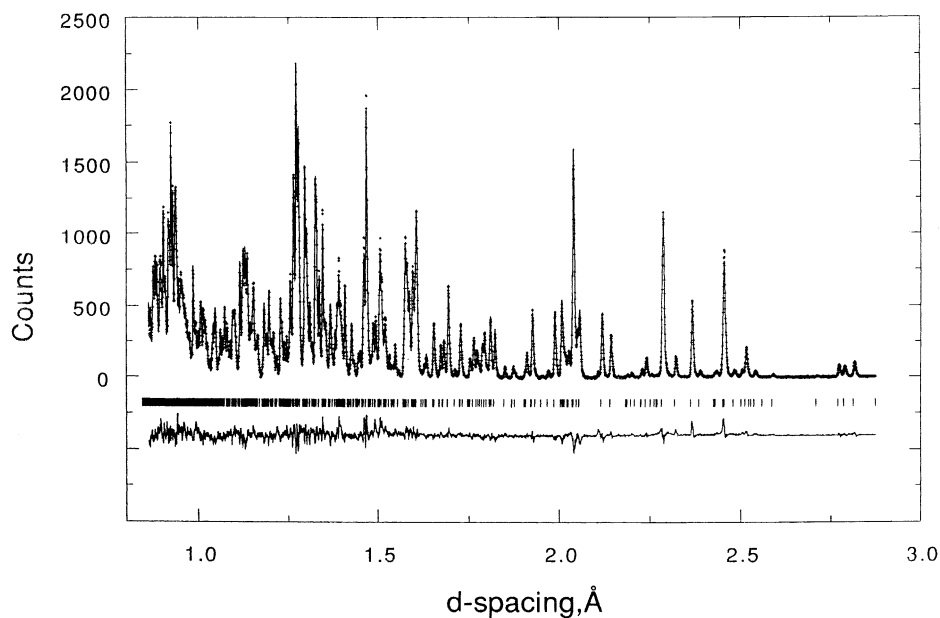
Fig. 1. Observed (+), calculated (solid line) and difference (below) neutron diffraction patterns for $Mg_{2.5}VMoO_8$. The tic marks indicate the allowed reflections in *Pnma*.

(Mg(2), Mn(2) and Zn(1)) were constrained to be 75% occupied, and (ii) all remaining sites were constrained to be fully occupied. The sum of vanadium and molybdenum is restrained by the second criteria, but the ratio of the two elements is not restrained in any way. These constraints reflect that in order to achieve charge neutrality for the stoichiometry $M_{2.5}VMoO_8$ there are cation vacancies. These vacancies are disordered on the Zn(1), Mn(2) and Mg(2) sites, which form chains of face-shared octahedra, in order to reduce cation–cation repulsion. However, these vacancies

are likely adjacent to clusters of three occupied sites along individual chains but lack correlation between chains. In all three cases, the refined stoichiometry is within 2% of the nominal formula, which verifies the validity of the refinement model and the constraints used. For $Mg_{2.5}VMoO_8$ and $Mn_{2.5}VMoO_8$, the refined occupancies of the two crystallographically unique tetrahedral sites are shown in Tables 2 and 3, respectively. The V^{5+} and Mo^{6+} cations are almost completely disordered, in close agreement with the single crystal studies [9,10] in which the disordered model was
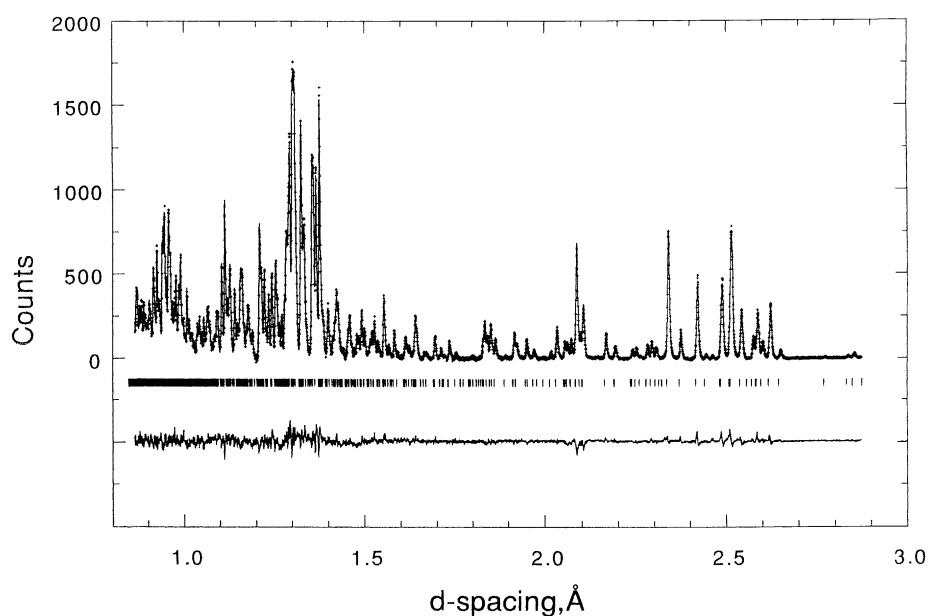

Fig. 2. Observed (+), calculated (solid line) and difference (below) neutron diffraction patterns for $Mn_{2.5}VMoO_8$. The tic marks indicate the allowed reflections in *Pnma*.

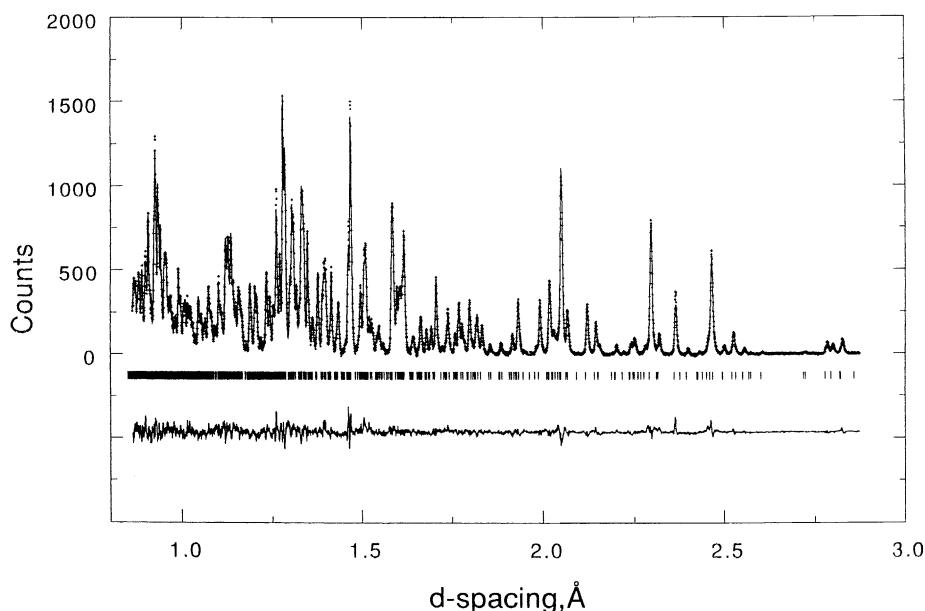Fig. 3. Observed (+), calculated (solid line) and difference (below) neutron diffraction patterns for $Zn_{2.5}VMoO_8$. The tic marks indicate the allowed reflections in $P2_12_12_1$.

elected based on the Hamilton test [23]. For $Zn_{2.5}VMoO_8$, there are three unique crystallographic sites, but the occupancies of V^{5+} and Mo^{6+} can still be calculated from the effective site scattering length based on the assumption that the three tetrahedral sites are fully occupied by some allocation of vanadium and molybdenum. The results are given in Table 4. V and Mo are essentially disordered on the three sites. However, V cations show a small preference for the

third site, again in agreement with the X-ray single crystal study [11]. Refinements of low temperature data (50, 150 and 250 K) with Pnma and $P2_12_12_1$ models indicate that the space group of $Zn_{2.5}VMoO_8$ remains $P2_12_12_1$ between 50 and 293 K.

The formation of $Mg_{2.5+x}V_{1+2x}Mo_{1-x}O_8$ ($x \neq 0$) was examined using powder XRD. Diffraction patterns of the samples calcined for 12 h at various temperatures

Table 4
Atomic parameters for $Zn_{2.5}VMoO_8$[a]

Atom	Wyckoff	x	y	z	$100 \times U_{iso}$	Occupancy
V(1)	4a	0.215(1)	0.740(1)	0.8082(3)	1.1(1)	0.474(12)
Mo(1)	4a	0.215(1)	0.740(1)	0.8082(3)	1.1(1)	0.526(12)
V(2)	4a	0.737(3)	0.015(1)	0.9070(8)	1.1(1)	0.501(17)
Mo(2)	4a	0.737(3)	0.015(1)	0.9070(8)	1.1(1)	0.499(17)
V(3)	4a	0.712(3)	0.472(1)	0.9065(7)	1.1(1)	0.552(4)
Mo(3)	4a	0.712(3)	0.472(1)	0.9065(7)	1.1(1)	0.448(4)
Zn(1)	4a	0.408(1)	0.751(2)	0.9995(5)	7.2(2)	0.75
Zn(2)	4a	0.253(1)	0.246(1)	0.9434(3)	2.7(1)	1
Zn(3)	4a	0.252(2)	0.0698(6)	0.7795(4)	2.1(2)	1
Zn(4)	4a	0.754(2)	0.9110(6)	0.7227(4)	1.9(2)	1
O(1)	4a	0.930(2)	0.1201(7)	0.9576(4)	2.3(2)	1
O(2)	4a	0.917(2)	0.9798(7)	0.8213(4)	2.6(2)	1
O(3)	4a	0.433(2)	0.1033(6)	0.8736(4)	1.7(2)	1
O(4)	4a	0.641(2)	0.8798(7)	0.9504(4)	1.6(2)	1
O(5)	4a	0.420(2)	0.8769(7)	0.7839(5)	2.6(2)	1
O(6)	4a	0.1404(9)	0.744(1)	0.8997(2)	2.1(1)	1
O(7)	4a	0.417(2)	0.6090(5)	0.7897(4)	0.6(2)	1
O(8)	4a	0.9397(8)	0.7423(8)	0.7420(2)	1.9(1)	1
O(9)	4a	0.658(2)	0.6030(7)	0.9564(4)	2.9(3)	1
O(10)	4a	0.918(2)	0.4925(5)	0.8303(3)	1.6(2)	1
O(11)	4a	0.918(2)	0.3629(6)	0.9683(4)	2.1(2)	1
O(12)	4a	0.432(2)	0.3737(6)	0.8830(4)	0.8(2)	1

[a] The unit cell of the zinc analogue is shifted one quarter unit in the z-direction relative to those of the other two structures and the thermal parameters were constrained to be equal.
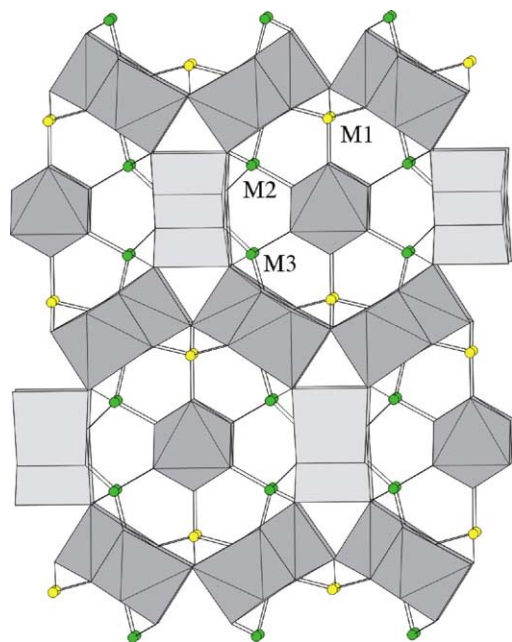
Fig. 4. General structure for $M_{2.5}VMoO_8$ (M = Mg, Mn, Zn). The small circles marked Mi, M2 and M3 are the V/Mo sites. MO_6 polyhedra are shown as dark grey octahedra and light grey trigonal prisms.

revealed that a mixture of $Mg_3(VO_4)_2$ and $MgMoO_4$ was present in every sample calcined below 1173 K (Fig. 5). $Mg_{2.5}VMoO_8$ ($x = 0$) was detected at 1173 K. However, higher reaction temperatures were needed to begin forming the phases with excess vanadium ($x = 0.02, 0.04$) or excess molybdenum ($x = -0.02, -0.04$). $Mg_{2.5+x}V_{1+2x}Mo_{1-x}O_8$ was detected in all samples by 1223 K. Because many $Mg_{2.5+x}V_{1+2x}Mo_{1-x}O_8$ samples did not show evidence of forming at 1173 K after 12 h, a second set of experiments was conducted to determine if the $Mg_3(VO_4)_2$ and $MgMoO_4$ would react to form a single phase at 1173 K and longer reaction time. It was found that the $Mg_{2.5}VMoO_8$-type structure begins to form after 24 h of calcination. Single phase samples for the five compositions ($x = 0, \pm0.02$ and ±0.04) can be obtained by calcining at 1273 K for 24 h.

Investigation of the reaction of the precursors was performed by differential thermal analysis. Fig. 6 shows the DTA plots of the reactants that form $Mg_{2.5}VMoO_8$; each scan is offset by $1\,K\,mg^{-1}$ for clarification. The observed features shift to higher temperatures as the heating rates increase. Three exothermic peaks at approximately 550, 650, and 700 K were detected. These peaks correspond to the combustion of the organic compounds from the sol–gel

Table 5
Selected bond distances and angles for $Mg_{2.5}VMoO_8$, $Mn_{2.5}VMoO_8$ and $Zn_{2.5}VMoO_8$

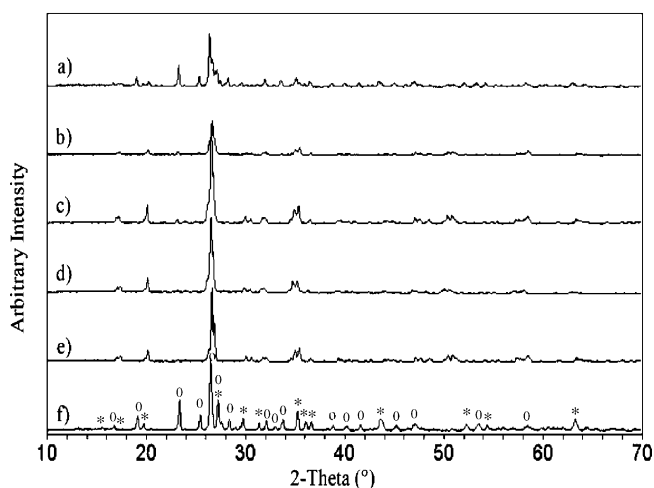|	$Mg_{2.5}VMoO_8$	$Mn_{2.5}VMoO_8$	$Zn_{2.5}VMoO_8$
Distances (Å)			
V/Mo(1)−O(5)	1.797(6)	1.827(7)	1.811(13)
V/Mo(1)−O(6)	1.764(4) × 2	1.744(4) × 2	1.651(8)
V/Mo(1)−O(7)	1.699(6)	1.664(6)	1.733(14)
V/Mo(1)−O(8)			1.813(8)
V/Mo(2)−O(1)	1.779(5)	1.766(5)	1.713(16)
V/Mo(2)−O(2)	1.704(4)	1.678(4)	1.800(15)
V/Mo(2)−O(3)	1.755(5)	1.784(5)	1.881(15)
V/Mo(2)−O(4)	1.790(4)	1.768(5)	1.672(15)
V/Mo(3)−O(9)			1.643(14)
V/Mo(3)−O(10)			1.708(14)
V/Mo(3)−O(11)			1.883(16)
V/Mo(3)−O(12)			1.792(14)
Angles (°)			
O(5)−V/Mo(1)−O(6)	108.1(2) × 2	107.6(3) × 2	109.8(8)
O(5)−V/Mo(1)−O(7)	116.4(3)	114.9(4)	103.8(4)
O(5)−V/Mo(1)−O(8)			105.9(6)
O(6)−V/Mo(1)−O(6)	105.0(3)	105.9(4)	
O(6)−V/Mo(1)−O(7)	109.4(2) × 2	110.3(3) × 2	109.9(7)
O(6)−V/Mo(1)−O(8)			116.7(4)
O(7)−V/Mo(1)−O(8)			109.9(7)
O(1)−V/Mo(2)−O(2)	110.7(2)	110.9(3)	106.2(5)
O(1)−V/Mo(2)−O(3)	105.0(2)	103.8(2)	108.2(5)
O(1)−V/Mo(2)−O(4)	108.4(2)	108.5(2)	117.7(5)
O(2)−V/Mo(2)−O(3)	110.3(2)	110.2(2)	104.4(5)
O(2)−V/Mo(2)−O(4)	113.5(2)	115.1(2)	110.9(5)
O(3)−V/Mo(2)−O(4)	108.1(2)	107.7(2)	108.5(5)
O(9)−V/Mo(3)−O(10)			114.5(5)
O(9)−V/Mo(3)−O(11)			106.5(5)
O(9)−V/Mo(3)−O(12)			117.8(5)
O(10)−V/Mo(3)−O(11)			101.0(5)
O(10)−V/Mo(3)−O(12)			111.7(5)
O(11)−V/Mo(3)−O(12)			102.9(5)

Fig. 5. Powder diffraction patterns for the metal oxides prepared using the sol–gel technique. The samples were calcined for 12 h at various temperatures until the $Mg_{2.5}VMoO_8$ structure was detected: (a) $Mg_{2.54}V_{1.08}Mo_{0.92}O_8$—1198 K; (b) $Mg_{2.52}V_{1.04}Mo_{0.96}O_8$—1198 K; (c) $Mg_{2.5}VMoO_8$—1173 K; (d) $Mg_{2.48}V_{0.96}Mo_{1.04}O_8$—1198 K; (e) $Mg_{2.46}V_{0.92}Mo_{1.08}O_8$—1223 K; (f) 1:2 molar mixture of $Mg_3(VO_4)_2$ (*) and $MgMoO_4$ (◯) 1148 K (shown for reference). The diffraction patterns were taken at ambient temperature in air.

precursors and the formation of a mixture of $MgMoO_4$ and $Mg_3(VO_4)_2$. The high temperature region (900–1373 K) shows little information about the reaction. As expected and discussed in the previous paragraph, $Mg_{2.5}VMoO_8$ is detected by powder XRD after reaction at 1223 K.

The $Mg_{2.5}VMoO_8$ ($x = 0$) structure begins to form at an appreciable rate at 1173 K. This is consistent with the phase diagram previously published [9]. Although a variety of factors can affect the kinetics of a solid-state reaction, such as the choice of reactants, the homogeneity of the reactants and diffusion, we observe that the phase forms approx-
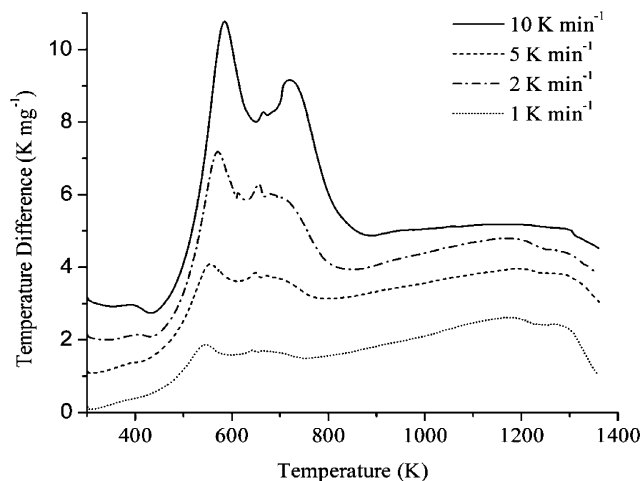
imately 250 K below its melting point (1423 K) [9]. Others have reported similar results. For example, the isostructural zinc compound has been reported by Kurzawa and Boasacka to form at approximately 300 K below its melting point (1118 K) at 823 K [24,25]. It is not surprising that López Nieto and co-workers did not detect the formation of the $Mg_{2.5}VMoO_8$ structure at 1173 K in their study [19]. Upon examination of their experimental conditions, it is apparent that a molybdenum precursor (aqueous ammonium heptamolybdate) was added, by the incipient wetness technique, to $Mg_3(VO_4)_2$ supported on MgO. Next the samples were calcined 873 K for 4 h and then at 1173 K for an unspecified time. Thus, it is probable that their reaction conditions were at too low of temperature and too short a time to allow the constituents to diffuse and react.

4. Conclusion

Neutron powder diffraction is an excellent technique to investigate the disorder between vanadium and molybdenum in multicomponent vanadomolybdates. The present neutron study verifies previous X-ray studies on the $M_{2.5}VMoO_8$ family of compounds and suggests that X-ray studies on other vanadomolybdates can reliably indicate the site distribution of the high valent cations. Formation studies of $Mg_{2.5-x}V_{1-2x}Mo_{1+2x}O_8$ ($x = 0$, ±0.02 and ±0.04) have shown that these phases do not form at an appreciable rate below 1173 K and a non-equilibrium mixture of $Mg_3(VO_4)_2$ and $MgMoO_4$ co-exist below this temperature. The high temperature required for the formation of $Mg_{2.5}VMoO_8$ combined with results from other studies demonstrates that the reaction is limited by solid-state diffusion.

Fig. 6. Differential thermal analysis plots of $Mg_{2.5}VMoO_8$. The plots were offset by 1 K mg^{-1} for clarity. The heating profiles consisted of: (a) 10 K min^{-1}; (b) 5 K min^{-1}; (c) 2 K min^{-1}; (d) 1 K min^{-1}. The plots were taken in air from ambient temperature to 1173 K.

References

[1] F. Cavani, F. Trifiro, Catal. Today 24 (1995) 307–313.
[2] E.A. Mamedov, V. Cortes Corberan, Appl. Catal. A 127 (1995) 1–40.

[3] M.M. Bettahar, G. Costentin, L. Savary, J.C. Lavalley, Appl. Catal. A 145 (1996) 1–48.

[4] S. Albonetti, F. Cavani, F. Trifiro, Catal. Rev.-Sci. Eng. 38 (1996) 413–438.

[5] T. Blasco, J.M. Lopez Nieto, Appl. Catal. A 157 (1997) 117–142.

[6] H.H. Kung, M.C. Kung, Appl. Catal. A 157 (1997) 105–116.

[7] W.D. Harding, H.H. Kung, V.L. Kozhevnikov, K.R. Poeppelmeier, J. Catal. 144 (1993) 597–610.

[8] J.D. Pless, D. Ko, R.R. Hammond, B.B. Bardin, P.C. Stair, K.R. Poeppelmeier, submitted for publication.

[9] X. Wang, C.L. Stern, K.R. Poeppelmeier, J. Alloys Compd. 243 (1996) 51–58.

[10] X. Wang, K.R. Heier, C.L. Stern, K.R. Poeppelmeier, J. Alloys Compd. 267 (1998) 79–85.

[11] X. Wang, K.R. Heier, C.L. Stern, K.R. Poeppelmeier, J. Alloys Compd. 255 (1997) 190–194.

[12] X. Wang, D.A. Vander Griend, C.L. Stern, K.R. Poeppelmeier, Inorg. Chem. 39 (2000) 136–140.

[13] B. Darriet, J. Galy, J. Solid State Chem. 8 (1973) 189–194.

[14] B. Darriet, J. Galy, Bull. Soc. Fr. Miner. Crystallogr. 91 (1968) 325–331.

[15] R. Kozlowski, K.J. Stadnicka, Solid State Chem. 39 (1981) 271–276.

[16] L. Kihlborg, Acta Chem. Scand. 21 (1967) 2495–2502.

[17] A.J.C. Wilson, International Tables for Crystallography, vol. C, first ed., Kluwer Academic Publishers, Dordrecht/Boston/London, 1995.

[18] V.G. Zubkov, I.A. Leonidov, K.R. Poeppelmeier, V.L.J. Kozhevnikov, Solid State Chem. 111 (1994) 197–201.

[19] A. Dejoz, J.M. Lopez Nieto, F. Marquez, M.I. Vazquez, Appl. Catal. A 180 (1999) 83–94.

[20] J.D. Jorgensen, J. Faber Jr., J.M. Carpenter, R.K. Crawford, J.R. Haumann, R.L. Hitterman, R. Kleb, G.E. Ostrowski, F.J. Rotella, T.G. Worlton, J. Appl. Crystallogr. 22 (1989) 321–333.

[21] A.C. Larson, R.B. Von Dreele, General Structure Analysis System (GSAS), Los Alamos National Laboratory Report LAUR, 1994.

[22] R.B. Von Dreele, J.D. Jorgensen, C.G. Windsor, J. Appl. Crystallogr. 15 (1982) 581–589.

[23] W.C. Hamilton, Acta Cryst. 18 (1965) 502–510.

[24] M. Kurzawa, M. Bosacka, J. Therm. Anal. Calorim. 64 (2001) 1081–1085.

[25] P. Tabero, M. Bosacka, M.J. Kurzawa, Therm. Anal. Calorim. 65 (2001) 865–869.